Spectroscopy of geoneutrinos with Borexino

Journal of Physics: Conference Series **2156** (2022) 012140 doi:10.1088/1742-6596/2156/1/012140

Spectroscopy of geoneutrinos with Borexino

Sindhujha Kumaran*

IKP-2, Forschungszentrum Jülich, 52428, Jülich, Germany
Physikalisches Institut III B, RWTH Aachen University, 52062, Aachen, Germany

E-mail: s.kumaran@fz-juelich.de

***On behalf of the Borexino collaboration**

M Agostini, K Altenmüller, S Appel, V Atroshchenko, Z Bagdasarian, D Basilico, G Bellini, J Benziger, D Bick, G Bonfini, D Bravo, B Caccianiga, F Calaprice, A Caminata, L Cappelli, P Cavalcante, F Cavanna, A Chepurnov, K Choi, D D'Angelo, S Davini, A Derbin, A Di Giacinto, V Di Marcello, X F Ding, A Di Ludovico, L Di Noto, I Drachnev, G Fiorentini, A Formozov, D Franco, F Gabriele, C Galbiati, M Gschwender, C Ghiano, M Giammarchi, A Goretti, M Gromov, D Guffanti, C Hagner, E Hungerford, Aldo Ianni, Andrea Ianni, A Jany, D Jeschke, S Kumaran, V Kobychev, G Korga, T Lachenmaier, T Lasserre, M Laubenstein, E Litvinovich, P Lombardi, I Lomskaya, L Ludhova, G Lukyanchenko, L Lukyanchenko, I Machulin, F Mantovani, G Manuzio, S Marcocci, J Maricic, J Martyn, E Meroni, M Meyer, L Miramonti, M Misiaszek, M Montuschi, V Muratova, B Neumair, M Nieslony, L Oberauer, A Onillon, V Orekhov, F Ortica, M Pallavicini, L Papp, Ö Penek, L Pietrofaccia, N Pilipenko, A Pocar, G Raikov, M.T Ranalli, G Ranucci, A Razeto, A Re, M Redchuk, B Ricci, A Romani, N Rossi, S Rottenanger, S Schönert, D Semenov, M Skorokhvatov, O Smirnov, A Sotnikov, V Strati, Y Suvorov, R Tartaglia, G Testera, J Thurn, E Unzhakov, A Vishneva, M Vivier, R.B Vogelaar, F von Feilitzsch, M Wojcik, M Wurm, O Zaimidoroga, S Zavatarelli, K Zuber and G Zuzel

Abstract. Borexino is a 280-ton liquid scintillator detector located at the Laboratori Nazionali del Gran Sasso (LNGS), Italy and is one of the two detectors that has measured geoneutrinos so far. The unprecedented radio-purity of the scintillator, the shielding with highly purified water, and the placement of the detector at 3800 m w.e. depth have resulted in very low background levels, making Borexino an excellent apparatus for geoneutrino measurements. This article will summarize the recent geoneutrino analysis and results with Borexino, from the period December 2007 to April 2019. The updated statistics and the optimized analysis techniques such as an increased fiducial volume and sophisticated cosmogenic vetoes, have led to more than a two-fold increase in exposure when compared to the previous measurement in 2015, resulting in a significant improvement in the precision. In addition, Borexino has also been able to reject the null hypothesis of the mantle geoneutrino signal with 99% C.L., for the first time, by exploiting the extensive knowledge of the crust surrounding the detector. This article will also include other geological interpretations of the obtained results such as the calculation of the radiogenic heat and the comparison of the results to various predictions. Additionally, upper limits for a hypothetical georeactor that might be present at different locations inside the Earth will also be discussed.

1. Introduction

The Earth's radioactivity leads to the emission of geoneutrinos. These electron (anti)neutrinos are produced from decays of long-lived isotopes, called Heat Producing Elements (HPEs):

$$^{238}\mathrm{U} \rightarrow {}^{206}\mathrm{Pb} + 8\alpha + 8e^- + 6\bar{\nu}_e + 51.7\,\mathrm{MeV} \quad (1)$$

$$^{235}\mathrm{U} \rightarrow {}^{207}\mathrm{Pb} + 7\alpha + 4e^- + 4\bar{\nu}_e + 46.4\,\mathrm{MeV} \quad (2)$$

$$^{232}\mathrm{Th} \rightarrow {}^{208}\mathrm{Pb} + 6\alpha + 4e^- + 4\bar{\nu}_e + 42.7\,\mathrm{MeV} \quad (3)$$

$$^{40}\mathrm{K} \rightarrow {}^{40}\mathrm{Ca} + e^- + \bar{\nu}_e + 1.31\,\mathrm{MeV}\ (89.3\%) \quad (4)$$

$$^{40}\mathrm{K} + e^- \rightarrow {}^{40}\mathrm{Ar} + \nu_e + 1.505\,\mathrm{MeV}\ (10.7\%) \quad (5)$$

The geoneutrino flux on Earth is about $10^6 \mathrm{cm}^{-2}\mathrm{s}^{-1}$. Direct geoneutrino measurements help answer several geological questions such as the abundance and distribution of HPE's inside the Earth, the contribution of radiogenic heat to the total surface heat flux measured on Earth (47 ± 2 TW), mantle properties, the Th/U ratio, and also test other hypotheses such as the presence of a georeactor.

Borexino is a liquid scintillator (LS) neutrino detector located at the Gran Sasso laboratory in Italy [2] and is one of the two detectors that has been able to measure geoneutrinos so far. It has a high light yield of about 500 p.e. per MeV, with an energy resolution of 5% at 1 MeV. In a LS detector, geoneutrinos interact via the Inverse Beta Decay (IBD) reaction: $\bar{\nu}_e + p \rightarrow e^+ + n$. The *prompt* signal is given by the positron, composed of the excess kinematic energy of the incident antineutrino after the 1.8 MeV kinematic threshold of the IBD, as well as the energy of the two 0.511 MeV gammas from annihilation. The prompt spectrum is thus directly correlated with the energy of the geoneutrinos. The *delayed* signal is given by the neutron which is captured after some time ($\sim$254.5 μs), on free protons (2.2 MeV gamma) or in about 1% of cases on ^{12}C atoms (4.95 MeV gamma) in the LS. The IBD threshold allows for the detection of geoneutrinos coming from only the ^{238}U and ^{232}Th decays. Geoneutrino signal is expressed in Terrestrial Neutrino Units (TNU), i.e. 1 antineutrino event detected via IBD over 1 year by a detector with 100% detection efficiency containing 10^{32} free target protons (roughly corresponds to 1 kton of LS). The expected geoneutrino signal at LNGS with respect to the antineutino energy is shown in Figure 1.

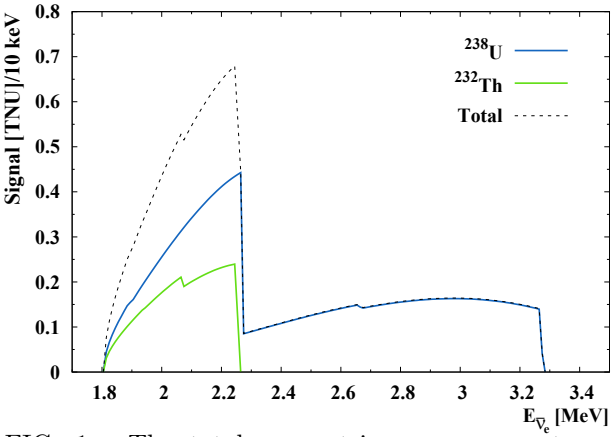

FIG. 1. The total geoneutrino energy spectrum expected to be detected at LNGS via IBD interaction on free proton (black dashed lines) [1].

2. Analysis strategy and methods

This section summarizes the optimized data selection cuts, the relevant backgrounds, and the systematic effects that were included in the Borexino geoneutrino analysis. The energy threshold of the prompt event was chosen according to IBD threshold of 1.8 MeV. The neutron captures on both protons and on ^{12}C atoms were included for the delayed signal, leading to the selection of two energy windows for the delayed event. In addition, space-time coincidence windows were also optimized to increase the signal-to-background ratio and suppress backgrounds as much as possible. The time difference between the prompt and delayed signals was chosen to be about five times the neutron capture time. Two different time windows were selected for different types

of events: double cluster events falling in the small 2.5-12.5 μs window and single cluster events falling in the 20-1280 μs. The distance between the prompt and delayed events was optimized using sensitivity studies to be 1.3 m. Muons and muon daughters (neutrons, ^{9}Li) were suppressed using complex time and space vetoes. A 2 ms time veto was applied to muons that pass only through the outer detector. For muons passing through both the inner and outer detectors, three different time vetoes (2 ms, 1.6 s, 2 s) and an additional spatial veto (whole detector or cylinder of radius 3 m around the muon) were applied depending on the type of muon. A fiducial volume cut was also applied to suppress background events originating from the inner vessel. The prompt event was required to be least 10 cm from the inner vessel. An α/β discrimination cut was applied to the delayed event to select only β-like events. Finally, a multiplicity cut was also applied. This cut makes sure that there are no high energy events (>400 p.e.) 2 ms before prompt, 2 ms after delayed, and in between the prompt and delayed events.

Reactor antineutrinos constitute the most important background for the geoneutrino analysis and they come from approximately 440 nuclear reactors around the world. Their flux can be calculated using the nominal reactor powers form the International Atomic Energy Agency (IAEA), the survival probability of neutrinos, and the neutrino oscillation parameters. The expected reactor antineutrino signal at LNGS according to this calculation is $84.5^{+1.5}_{-1.4}$ TNU and $79.6^{+1.4}_{-1.3}$ TNU, for without and with the 5 MeV "excess" observed by different reactor antineutrino experiments [3], respectively. The relevant non-antineutrino backgrounds are: (1) ^{9}Li background from muon spallation in the LS that remain after the time and spatial muon vetoes, (2) accidental coincidences due to the correlation of random events in space and time, and (3) (α,n) background arising from small amounts of radioactive ^{210}Po in the LS. The total number of expected non-antineutrino backgrounds is (8.28 ± 1.01) events and each source and the corresponding value is reported in Table I.

TABLE I. The expected number of events from non-antineutrino backgrounds in the IBD candidate sample of Borexino (exposure $\mathcal{E}_p$ = (1.29 ± 0.05) $\times 10^{32}$ protons × yr). The limits are 95% C.L [1].

Background Type	Events
^{9}Li background	3.6 ± 1.0
Untagged muons	0.023 ± 0.007
Fast n's (μ in WT)	<0.013
Fast n's (μ in rock)	<1.43
Accidental coincidences	3.846 ± 0.017
(α, n) in scintillator	0.81 ± 0.13
(α, n) in buffer	<2.6
(γ, n)	<0.34
Fission in PMTs	<0.057
^{214}Bi-^{214}Po	0.003 ± 0.001
Total	8.28 ± 1.01

An unbinned-likelihood spectral fit of the energy (charge variable) of all the prompt events was performed to obtain the geoneutrino signal at LNGS. Probability Density Functions (PDFs) constructed using Monte-Carlo (MC) of all spectral components were used for this, with the exception for the accidental coincidences background that was measured with sufficient precision using off-time coincidences in data. The spectral fit results in the number of events arising from each component. The fit is typically performed in the photoelectron range of 408–4000 (≈0.8–8 MeV). The number of geoneutrinos is always left free to vary to obtain a measurement. ^{232}Th and ^{238}U contributions can also be fit as two independent contributions, however Borexino has no sensitivity to measure them independently. The number of reactor antineutrino events is also left free to vary in most configurations. The three main non-antineutrino backgrounds are constrained using additional multiplicative Gaussian pull terms in the likelihood function. The resulting number of detected geoneutrinos and reactor antineutrinos are then expressed in the units of TNU, using the exposure and detection efficiency.

The systematic sources of uncertainties included for the final results are: atmospheric neutrino background, reactor antineutrino spectral shapes with and without the "5 MeV excess", inner vessel shape reconstruction, MC detection efficiency, and position reconstruction resolution.

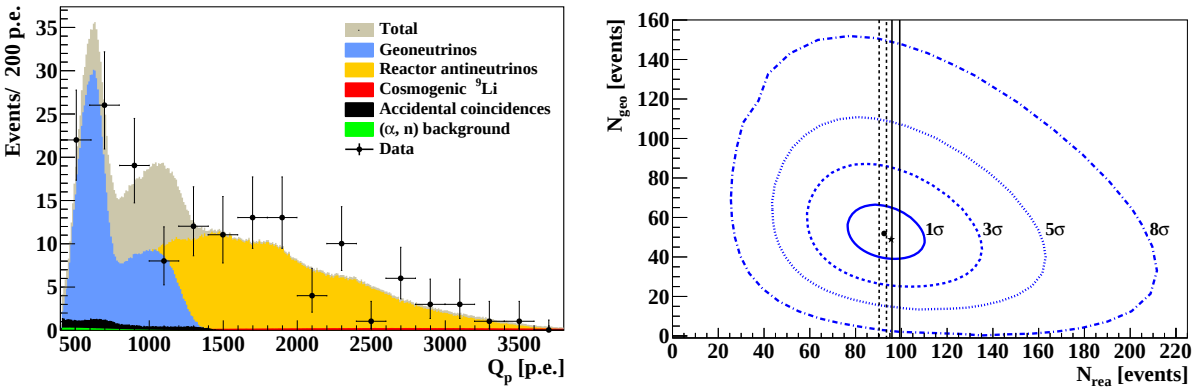

(a) (b)

FIG. 2. Spectral fit results from the analysis of 154 golden IBD candidates. (**a**) Spectral fit of the data (black points with Poissonian errors) assuming the chondritic Th/U ratio. The total fit function containing all signal and background components is shown in grey. Geoneutrinos (blue) and reactor antineutrinos (yellow) were left free to vary in the fit. Other non-antineutrino backgrounds were constrained in the fit. (**b**) The best fit point (black dot) and the contours for the 2D coverage of 68, 99.7, (100–5.7×10^{-5})%, and (100–1.2×10^{-13})%, (corresponding to 1, 3, 5, and 8σ, respectively), for number of geoneutrinos (N_{geo}) versus number of reactor antineutrinos (N_{rea}), assuming Th/U chondritic ratio. The vertical lines mark the 1σ bands of the expected reactor antineutrino signal (solid-without "5 MeV excess", dashed-with "5 MeV excess"). For comparison, the star shows the best fit performed assuming the ^{238}U and ^{232}Th contributions as free and independent fit components [1].

3. Results and Conclusions

In the analysis period used between December 2007 and April 2019, 154 golden IBD candidates satisfied all the above-mentioned data selection cuts. The geoneutrino signal was extracted from the previously described unbinned likelihood fit. The resulting number of geoneutrinos was $52.6^{+9.4}_{-8.6}\,(\text{stat})^{+2.7}_{-2.1}\,(\text{sys})$ (68% interval) corresponding to a signal of $47.0^{+8.4}_{-7.7}\,(\text{stat})^{+2.4}_{-1.9}\,(\text{sys})$ TNU. The reactor antineutrino signal from the spectral fit was found to be compatible with the expectations, confirming the ability of Borexino to measure antineutrinos. The resulting spectral fit and the 1, 3, 5, and 8σ contours for the number of geoneutrinos versus reactor antineutrinos are shown in Figure 2. The spectral fit performed by leaving the ^{238}U and ^{232}Th contributions free also yielded compatible results.

The mantle signal was also extracted from a similar spectral fit, but the relatively well-known contribution from the bulk lithosphere was constrained as $28.8^{+5.5}_{-4.6}$ events, corresponding to an expected signal of $25.9^{+4.9}_{-4.1}$ TNU. The MC PDFs of both the mantle and lithosphere were constructed from the PDFs of ^{232}Th and ^{238}U geoneutrinos. The lithospheric PDF was scaled using the geologically observed Th/U signal ratio of 0.29. The applied Th/U signal ratio to the mantle PDF was 0.26, so as to maintain the chondritic Th/U mass ratio of 3.9 for the bulk Earth [1]. Both the mantle and reactor antineutrino contributions were left free to vary in the fit. The data energy points and the different MC PDFs used in the fit are shown in Figure 3(a). The final mantle signal obtained was $21.2^{+9.5}_{-9.0}\,(\text{stat})^{+1.1}_{-0.9}\,(\text{sys})$ TNU, after the addition of the systematic uncertainties. MC pseudo-experiments with and without a generated mantle signal, were used to study the statistical significance of the mantle geoneutrino signal. This method allowed for the rejection of the null-hypothesis of the mantle signal with 99.0% C.L. (corresponding to 2.3σ significance).

The extracted mantle signal can be converted to a radiogenic heat production of $24.6^{+11.1}_{-10.4}$ TW (68% C.I.). Despite the compatibility of Borexino results with different Earth models, a $\sim$2.4σ tension was observed with models that predict the lowest concentration of HPEs in the mantle.

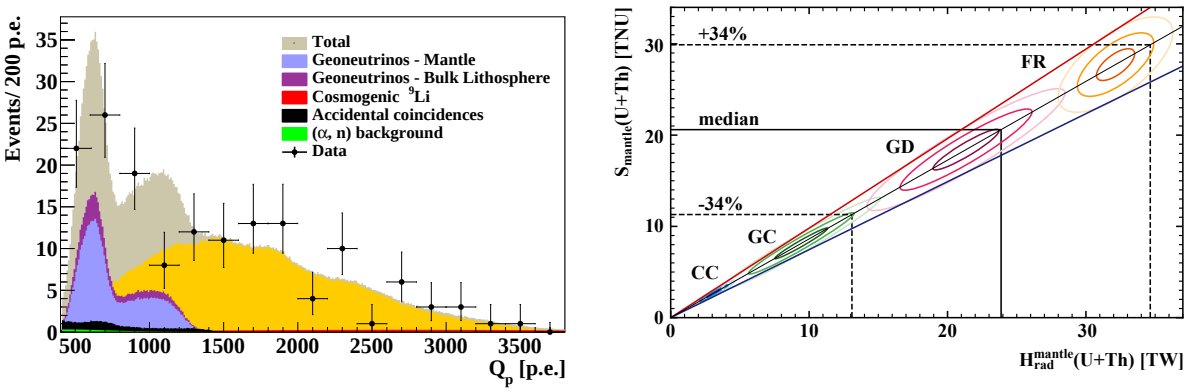

(a) (b)

FIG. 3. (a) Spectral fit used for the extraction the mantle signal, after constraining the bulk lithosphere contribution. The summed PDFs of all the signal and background components is shown by the grey shaded band [1]. (b) Expected Mantle geoneutrino signal in Borexino with respect to the U and Th mantle radiogenic heat: the area between the red and blue lines denotes the full signal-heat window allowed between a homogeneous mantle (low scenario) and a unique rich layer just above the Core-Mantle Boundary (CMB) (high scenario). The average of the slopes of the blue and red lines is given by the central black line. The blue, green, red, and yellow ellipses are calculated with the U and Th mantle radiogenic power according to different BSE models Cosmochemical (CC), Geochemical (GC), Geodynamical (GD), and Fully Radiogenic (FR) Earth. For each model, darker to lighter shades of respective colours represent 1, 2, and 3σ contours. The the mantle signal measured by Borexino is given by black horizontal lines: black horizontal lines represent. the median mantle signal (solid line) and the 68% coverage interval (dashed lines) [1].

This comparison is shown in Figure 3(b). Using the assumption of 18% contribution from ^{40}K in the mantle and the lithospheric heat contribution of $8.1^{+1.9}_{-1.4}$ TW, the estimate on the total radiogenic heat of the Earth using Borexino is $38.2^{+13.6}_{-12.7}$ TW. Through this measurement, the mantle HPE composition can be constrained additionally as: $a_{\mathrm{mantle}}(\mathrm{U}) > 13$ ppb and $a_{\mathrm{mantle}}(\mathrm{Th}) > 48$ ppb with 95% C.L. The mantle radiogenic heat power can also be constrained as $H^{\mathrm{mantle}}_{\mathrm{rad}}(\mathrm{U{+}Th}) > 10$ TW and $H^{\mathrm{mantle}}_{\mathrm{rad}}(\mathrm{U{+}Th{+}K}) > 12.2$ TW, and the convective Urey ratio can be constrained as $UR_{CV} > 0.13$ with 95% C.L.

Upper limits on the signal from a hypothetical georeactor inside the Earth were also obtained after constraining the number of expected reactor antineutrino events, due to the degeneracy of their spectral shapes. The existence of a georeactor with a power greater than 0.5/2.4/5.7 TW was excluded at 95% C.L., assuming its distance from the detector to be at 2900/6371/9842 km.

References

[1] Agostini M *et al.* (Borexino Collaboration) 2020 *Physical Review D* **101** 012009
[2] Alimonti G *et al.* (Borexino Collaboration) 2009 *Nuclear Instruments and Methods A* **600** 568–93
[3] An F. P. *et al.* (Daya Bay Collaboration) 2017 *Physical Review Letters* **118** 251801